

ChemComm

Accepted Manuscript



This is an *Accepted Manuscript*, which has been through the Royal Society of Chemistry peer review process and has been accepted for publication.

Accepted Manuscripts are published online shortly after acceptance, before technical editing, formatting and proof reading. Using this free service, authors can make their results available to the community, in citable form, before we publish the edited article. We will replace this *Accepted Manuscript* with the edited and formatted *Advance Article* as soon as it is available.

You can find more information about *Accepted Manuscripts* in the [Information for Authors](#).

Please note that technical editing may introduce minor changes to the text and/or graphics, which may alter content. The journal's standard [Terms & Conditions](#) and the [Ethical guidelines](#) still apply. In no event shall the Royal Society of Chemistry be held responsible for any errors or omissions in this *Accepted Manuscript* or any consequences arising from the use of any information it contains.

Dynameric Asymmetric Membranes for Directional Water Transport

Received 00th January 20xx,
Accepted 00th January 20xx

Yan Zhang, Mihail Barboiu*

DOI: 10.1039/x0xx00000x

www.rsc.org/

Hydrophilic/hydrophobic dynamers prepared via template partial phase segregation, have been used for the formation of asymmetric membranes for directional water transport.

Dynamic polymers - Dynamers¹⁻⁴ have emerged as a new type of reversible materials giving access to adaptive behaviours in response to external⁵⁻¹¹ or internal stimuli, leading to the specific structures and of variable morphologies.¹²⁻¹³ Recently we became interested in biomimetic water transport which may imply important insights on solving important biological scenarios and also to provide an improvement over current technologies in water desalination.¹⁴⁻¹⁶ Wetting behaviours in natural systems (i.e. lotus leaves, butterfly wings *etc.*) are other inspiring examples for the construction of systems for water transport.¹⁷⁻²⁰ We know that the directional water transport can be achieved by using hydrophobic/hydrophilic HP/HY porous macroscopic layers.²⁰ Within this context, we considered that dynameric membranes prepared under molecular control⁶ may constitute an interesting alternative in the ability to control the directional water transport and to go further toward highly selective separations of low mass solutes (ions, peptides, etc) controlled via molecular diffusion.

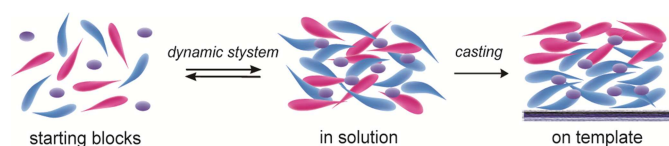


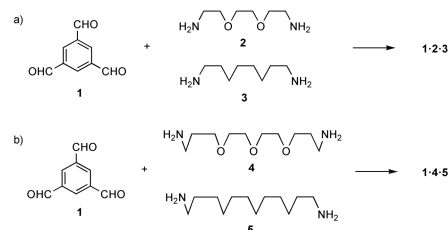
Figure 1. Constitutional segregation of the hydrophilic (blue) /hydrophobic (red) elements connected via core-centres (violet) for asymmetric membrane generation.

Herein, we report asymmetric HP/HY dynameric membranes for directional water transport. We presumed that the combination of HP and HY segments connected *via* reversible covalent bonds, may induce phase segregation at the

Institut Européen des Membranes, ENSCM-UM-CNRS, Adaptive Supramolecular Nanosystems Group, Place Eugène Bataillon, CC 047, F-34095 Montpellier, France.
Email: mihail-dumitru.barboiu@univ-montp2.fr

*Electronic Supplementary Information (ESI) available: NMR, SEM, EDX contact angle and water transport experiments. See DOI: 10.1039/x0xx00000x

molecular level in the presence of a templating support, under the pressure of constitutional internal affinity of components. In order to generate such dynamers, trialdehyde core-centres, HY PEG-diamine and HP alkane-diamine segments have been connected *via* reversible amino-carbonyl/imine chemistry. This results in the formation of dynameric frameworks, enabling the dynamic exchange between components in solution and gels toward the membrane formation by casting on templating support. Using such constitutional reorganization during the phase change processes,²¹ partial phase segregation can be achieved at molecular level (Fig. 1). Our initial attempt started from 1,3,5-benzenetrialdhyde, **1** and 2,2'-(ethylenedioxy)bis(ethylamine) **2**, (0.75 eq.) and 1,8-diamino-octane **3**, (0.75 eq.) building blocks (reflux 2h, in CHCl₃ -Scheme 1a). ¹H-NMR spectral data agree with the total consumption of aldehydes and the formation of symmetrical cross-linked **1-2-3** frameworks (Fig S3, S4 ESI). HP Teflon plates have been used as templating surfaces. In order to exam the molecular segregation effect, we used the contact angle analysis (CA) as direct indication of wettability behaviours, as well as energy-dispersive X-ray spectroscopy (EDX) to know the elemental distribution on both membrane surfaces. The CA show that the wettabilities of the membrane air-contact upside surface and down-side support-contact surface are almost similar: 80.9° and 88.0° (Teflon) or 76.7° and 80.2° (Glass) respectively. In agreement EDX atomic distribution (ESI) proving that for the precursors the constitutional interactions of the short chains are not enough strong in order to promote segregation.



Scheme 1. Schematic representation of the synthesis of dynameric frameworks combining a) 1,3,5-benzenetrialdhyde **1**, and 2,2'-(ethylenedioxy)bis(ethylamine) **2** and 1,8-diaminooctane **3** and b) 1,3,5-benzenetrialdhyde **1**, 4,7,10-trioxo-1,11-tridecanediamine **4**, and 1,12-diaminododecane **5**.

Considering the moderate segregation observed for **1-2-3**, longer molecular components **4,7**, 10-trioxa-1,13-tridecane-diamine **4** and 1,12-diamino-dodecane **5**, were used thereafter using similar experimental conditions (Scheme 1b). In this case, solvents with different polarities were screened: CHCl₃, CH₃CN, THF and acetone. ¹H-NMR spectral data agree with the partial consumption of aldehydes and the formation of unsymmetrical cross-linked **1-4-5** frameworks (Fig S5-S7 ESI). From the results of CA, all membranes **1-4-5** showed considerable improvement in phase segregation compared to **1-2-3**. For example with CHCl₃, contact angle of upside surface was 36.72°, and the value from down side surface was 71.90°. Besides this, for the membrane generated from CH₃CN, water disappeared quickly on the upside surface showing high wettability, while the contact angle of the down side of the membrane was 86.21°. Furthermore, the EDX data clearly demonstrated the uneven elemental distribution between the two sides (Table 1). However we note that the CA values are reminiscent with a partial segregation behavior as time as the HY CA are not very low and HP CA angles are not very high. Along the phase segregation process, the hydrophilic amino and PEG groups were tend to gather together on the upside surface, leaving most of the hydrophobic alkane groups on the bottom downside surface, in contact with the hydrophobic Teflon template. HY/HP and HY/HP dominant/residual behaviors are generated at the molecular level toward the hybrid distinct surfaces of the material. We noted that the difference between membrane upside and downside surfaces is a general trend and strongly dependent of the used solvent (Table 1).

Table 1. EDX result for membranes generated from different solvents.

		CA ^a	C ^b	N	O
CH ₃ CN	upside	- ^c	78.14	10.62	11.24
	down side	86.2°	83.45	9.68	6.87
CHCl ₃	upside	36.7°	87.87	2.40	9.73
	down side	71.9°	89.11	1.55	9.34
THF	upside	49.6°	78.82	10.97	10.21
	down side	65.3°	80.82	10.57	8.61
acetone	upside	40.6°	72.82	15.22	11.96
	down side	80.4°	75.71	13.70	10.58

^a Contact angles were measured by water droplets on the surface of the membrane; ^b the recorded data are atomic % percentages; ^c water droplets disappeared quickly on the membrane surface.

The morphology from Scanning Electron Microscopy (SEM) further confirmed that membranes (100-200 μm thick) are dense without pinholes or pores. Among the solvents tested, the membrane generated from CH₃CN showed an important difference between the two sides of different morphological behaviors. Even from raw eyes, the upside of the membrane presented as rough surface, at the same time the down side of the membrane appeared as very smooth (Fig. 2). This interesting behavior is not only attributed to the polarity of CH₃CN, favoring the molecular segregation, but also to the kinetics of the evaporation process. The difference in the morphological surface behaviors is still present in the cases of the other solvents, resulting in the formation of less tortuous

non-porous upside surfaces (Fig. S9, ESI). Importantly the same experiment conducted for a mixture of **1-4** (molar ratio of 1:1.5) casted from CH₃CN, results in the formation of tight non-porous morphologies on the both sides, confirming the importance of molecular segregation in generating asymmetric morphologies (Fig. 2e-f). CA showed that water quickly disappeared from both sides of the membrane **1-4** and EDX gave almost the same elemental distribution of the two sides.

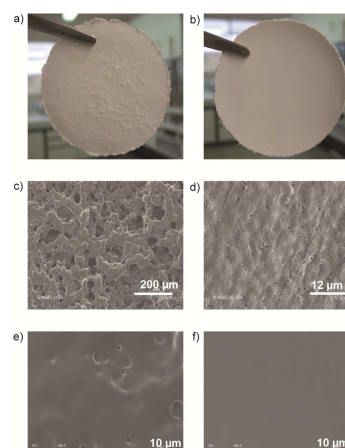


Figure 2. The images of upside (a) and down side (b) of the membrane **1-4-5**; the SEM images of the upside (c) and down side (d) of the membrane **1-4-5**; the SEM images of the upside (e) and down side (f) of the membrane **1-4** as comparison.

The membranes saturated in water for 2h have been evaluated for their transport properties by using a Sterlitech HP4750 stirred cell, connected with a balance to measure the water mass transported through the membrane. The total water mass versus time profiles have been used to determine the flux of water filtered through the membranes, oriented with upside or with downside surface to the water stream (Fig. 3). Interestingly, at low pressure of 0.007 bar, water is transported only when the upside surface of the membrane **1-4-5**, casted from CH₃CN is exposed to water, with a mass flux of 0.630 g/min (Fig. 3c), while is completely blocked from the down-side surface of the membrane (Fig. 3c). The water permeability is favored for the upside surface of the membrane ($P = 7400 \text{ L}\cdot\text{m}^{-2}\cdot\text{h}^{-1}\cdot\text{bar}^{-1}$). When higher pressures are applied, water fluxes are increasing and water can also slowly penetrate from the down-side ($P = 3900 \text{ L}\cdot\text{m}^{-2}\cdot\text{h}^{-1}\cdot\text{bar}^{-1}$). For the reference membrane **1-4** casted from CH₃CN we recorded similar permeabilities ($P = 18 \text{ L}\cdot\text{m}^{-2}\cdot\text{h}^{-1}\cdot\text{bar}^{-1}$ and $P = 14 \text{ L}\cdot\text{m}^{-2}\cdot\text{h}^{-1}\cdot\text{bar}^{-1}$ respectively) for the two sides (Fig. 3d). The membranes casted from other less polar solvents than CH₃CN give less different permeabilities between the two sides in accordance with CA and EDX data, showing less phase segregation at the molecular level (Table 2, Fig. S10, ESI). We point out on high values of water permeability obtained with these membranes that would make them as potential candidates for the separation of other solutes like, ions, peptides, proteins or other metabolites.²² The mechanism of water permeability is different to the related previous studies on porous systems,²⁰ and is mostly related to the wettability and to the dominant/residual HY/HP or HP/HY hydrophilic

structures of the dense surfaces. If water is dropped on the on dense non-porous HY surface, it spreads and absorb into the film. This effect is amplified by the roughness of the HY surface of the membrane **1-4-5**, casted from CH₃CN showing one/two orders of magnitude higher permeability than other membranes with smooth surfaces. Although the HP region would tend to block the water penetration, the increased accumulation of water in the HY region will then reach the residual HY channels of the HP part overcoming the hydrophobic forces and penetrating the whole membrane (Fig. 3e). Differently, the accumulation of water in the HY residual part of the HP region is probably not sufficient for reaching a critical water volume to overcome the hydrophobic forces and to penetrate the HY part of the membrane (Fig. 3f). However this blockage is overcome by increasing the operating pressure which increase the water permeability from HP side.

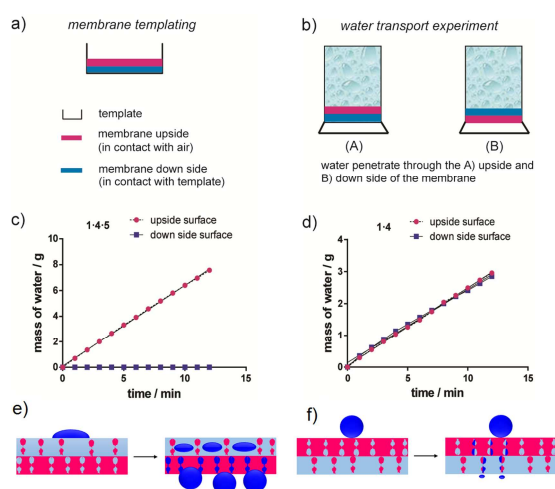


Figure 3. Water transport experiment for the two sides of membrane: schematic presenting of a) the membrane two sides and b) water transport directions; water flux of the two sides of the membrane c) **1-4-5** and d) **1-4**; Mechanism of preferential water permeation of e) wettable HY surface and of f) unwettable HP surface.

Table 2. Water permeability of **1-4-5** from different solvents and **1-4** from CH₃CN.^a

		upside surface ^b (L·m ⁻² ·h ⁻¹ ·bar ⁻¹)	down-side surface ^c (L·m ⁻² ·h ⁻¹ ·bar ⁻¹)
1-4-5	CH ₃ CN	7400	3900
	acetone	25	31
	CHCl ₃	160	71
1-4	CH ₃ CN	18	14

^a The calculation method see ESI; ^b water penetrate through the upside surface; ^c water penetrate through the down side surface.

All these results demonstrate that the synergetic incorporation of hydrophobic/hydrophobic components is crucial for the template induced phase segregation within the structure of the Dynameric frameworks for asymmetric membrane preparation. This process is strongly dependent of used solvent and is supported by CA, EDX and SEM, experimental results. Its application for directional water transport was further confirmed. At low pressure, water can only penetrate through HY side of the membrane and blocked from the HP side. Straightforward synthetic access to asymmetric

membranes give rise to novel strategies to constitutionally built up under molecular control very productive transport membranes for high added value applications as water purification or protein purification.

This work was supported by funds from ITN DYNANO, PITN-GA-2011-289033 (www.dynano.eu) and Agence National de Recherche, ANR-DYNAFUN.

Notes and references

1. J. Lehn, *Aust. J. Chem.*, 2010, **63**, 611-623.
2. J.-M. Lehn, *Angew. Chem., Int. Ed.*, 2013, **52**, 2836-2850.
3. R. Catana, M. Barboiu, I. Moleavin, L. Clima, A. Rotaru, E. Ursu, M. Pinteala, *Chem. Commun.* 2015, **51**, 2021-2024.
4. M. Barboiu, ed., *Constitutional Dynamic Chemistry*, Springer Verlag, Berlin, 2012.
5. T. Aida, E. W. Meijer and S. I. Stupp, *Science*, 2012, **335**, 815-817.
6. G. Nasr, M. Barboiu, T. Ono, S. Fujii and J.-M. Lehn, *J. Membr. Sci.*, 2008, **321**, 8-14.
7. N. Roy, E. Buhler and J.-M. Lehn, *Chem. Eur. J.*, 2013, **19**, 8814-8821.
8. J. Yang, Z. Li, Y. Zhou and G. Yu, *Polym. Chem.*, 2014, **5**, 664-6650.
9. E. Kolomiets and J.-M. Lehn, *Chem. Commun.*, 2005, 1511-1521.
10. S. Dong, Y. Luo, X. Yan, B. Zheng, X. Ding, Y. Yu, Z. Ma, C. Zhao and F. Huang, *Angew. Chem., Int. Ed.*, 2011, **50**, 1905-1909.
11. M. J. Barthel, T. Rudolph, A. Teichler, R. M. Paulus, J. Vitz, S. Hoepfner, M. D. Hager, F. H. Schacher and U. S. Schubert, *Adv. Funct. Mater.*, 2013, **23**, 4921-4931.
12. C.-F. Chow, S. Fujii and J.-M. Lehn, *Chem. Commun.*, 2005, 4363-4365.
13. D. Janeliunas, P. van Rijn, J. Boekhoven, C. B. Minkenbergh, H. van Esch and R. Eelkema, *Angew. Chem., Int. Ed.*, 2013, **52**, 1998-2001.
14. a) Y. Le Duc, M. Michau, A. Gilles, V. Gence, Y.-M. Legrand, J. van der Lee, S. Tingry, M. Barboiu, *Angew. Chem. Int. Ed.* 2011, **50**, 11366-11372; b) M. Barboiu, *Angew. Chem., Int. Ed.*, 2012, **51**, 11674-11676.
15. M. Barboiu and A. Gilles, *Acc. Chem. Res.*, 2013, **46**, 2814-2823.
16. M. Barboiu, *Eur. J. Inorg. Chem.*, 2015, **2015**, 1112-1125.
17. X. J. Feng and L. Jiang, *Adv. Mat.*, 2006, **18**, 3063-3078.
18. X. Yao, Y. Song and L. Jiang, *Adv. Mat.*, 2011, **23**, 719-734.
19. L. Jiang, Y. Zhao and J. Zhai, *Angew. Chem., Int. Ed.*, 2014, **116**, 4438-4441.
20. J. Wu, N. Wang, L. Wang, H. Dong, Y. Zhao and L. Jiang, *Soft Matter*, 2012, **8**, 5996-5999.
21. a) L. Marin, B. Simionescu, M. Barboiu, *Chem. Commun.* 2012, **48**, 8778-8780; b) S. Mihai, A. Cazacu, C. Arnal-Herault, G. Nasr, A. Meffre, A. van der Lee, M. Barboiu, *New. J. Chem.*, 2009, **33**, 2335-2343; c) L. Hu, Y. Zhang, O. Ramström, *Sci. Rep.* 2015, **5**, 11065; doi: 10.1038/srep11065.
22. A. Mehta, A.L. Zydney, *J. Membrane Sci.* 2005, **249**, 245-249.